On the applicability of multiaxial high cycle fatigue criteria to metallic materials

Roberta A. Gonçalves[1], *Marcos* V. Pereira[1,*] and *Fathi* A. Darwish[2]

[1] Catholic University of Rio de Janeiro, Department of Chemical and Materials Engineering, Rua Marques de São Vicente 225, 22453-901 Rio de Janeiro – RJ, Brazil.
[2]Fluminense Federal University, Department of Civil Engineering, Rua Passo da Patria 156, 24210-240 Niteroi – RJ, Brazil.

Abstract. A comparative study is made of the applicability of critical plane based multiaxial high cycle fatigue models to predicting the fatigue behavior of metallic materials. A number of models, namely Matake, McDiarmid, Carpinteri and Spagnoli, Liu and Mahadevan and Papadopoulos, were applied to fatigue limit states, involving synchronous fully reversed in-phase sinusoidal bend and torsion loading. The results obtained indicated a good predictive capability of the models with an average error index situated approximately between -5,5% and 4,5%. However, this average was limited to less than 3% for the latter three models. Finally, the critical plane orientation, which, for a given material, is characteristic of the proper model, is compared with that of the fracture plane, exclusively determined by the ratio between the shear stress and normal stress amplitudes.

1 Introduction

High cycle fatigue under uniaxial loading has shown that many metallic materials possess a fatigue limit, which means that they can sustain a very high (theoretically infinite) number of cycles without fatigue failure. However, many mechanical components, such as railroad wheels, crankshafts, axles and turbine blades are expected to experience multiaxial loading during their in-service lifetime. Accordinglly, the fatigue problem becomes more complex due to the complexity of the stress states, loading histories and different orientations of the initial crack in the components.

Generalization of the fatigue limit concept for multiaxial loading conditions is considered compatible with the idea of dividing the whole stress space in two parts, namely safe and unsafe. The safe part, which contains the origin, is bounded by a closed surface and the fatigue criterion can thus be expressed in terms of an inequality whose satisfaction signifies that the stress state induced by the external cyclic loading remains within the safe part of the stress space [].

Over many decades of research, a large number of models have been proposed to predict fatigue failure under multiaxial loading conditions. As the stress levels involved in high cycle fatigue are kept below the elastic limit, only stress based models, namely Matake (Ma) [1], McDiarmid (Mc) [2,3], Findley (F) [4], Carpinteri and Spagnole (C & S) [5-7], Liu and Mahadevan (L & M) [8] and Papadopoulos (P) [9,10] models, are to be considered in the present work. The underlying purpose is to test the applicability of these six models to some experimental loading conditions, available in the literature [11,12], involving synchronous fully reversed sinusoidal in-phase bend and torsion loading applied to a variety of metallic materials with different fatigue behaviors. At this point, it should be emphasized that all of the chosen loading conditions correspond to the fatigue limit state above which fatigue occurs and below which fatigue life extends over a very high number of cycles, in analogy with the fatigue limit state for uniaxial loading.

Whereas the use of Papadopoulos criterion requires only knowing the applied stress amplitudes, the other models depend for their application on the prior identification of the critical plane, where fatigue damage can occur leading to crack nucleation. Assuming that the critical plane is already known, the normal and shear stress amplitudes can be determined and fatigue failure assessment can thus be presented in the form of inequality. The relative difference between the two sides of the inequality is referred to as the error index and, for a given fatigue limit state, it can be null, positive or negative. As the fatigue criteria in question are to be applied simultaneously to a given loading condition, a comparison of the error index involved is expected to provide a good assessment of their predictive capabilities in defining the fatigue behavior.

Finally, the critical plane orientation, determined for each model, is presented in comparison with that of the fracture plane, for the loading conditions involved.

2 High cycle multiaxial fatigue criteria

The inequalities representative of the Matake, McDiamird, Findley, Carpinteri and Spangnoli, Liu and

* Corresponding author: marcospe@puc-rio.br

Mahadevan and Papadopoulos are given, respectively, by expressions (1) to (6):

$$C_a + \mu \, N_{max} \;\le t_{-1} \tag{1}$$

$$C_a + \frac{t_{-1}}{2\sigma_u} N_{max} \;\le t_{-1} \tag{2}$$

$$C_a + k \, N_{max} \;\le f \tag{3}$$

$$\sqrt{N_{max}^2 + (\frac{f_{-1}}{t_{-1}})^2 \, C_a^2} \;\le f_{-1} \tag{4}$$

$$\sqrt{[\frac{N_a + \left(1 + \eta \frac{N_m}{f_{-1}}\right)}{f_{-1}}]^2 + (\frac{C_a}{t_{-1}})^2} \;\le \lambda \tag{5}$$

$$\sqrt{\frac{\sigma_a^2}{3} + \tau_a^2} + \alpha \frac{\sigma_a + \sigma_m}{3} \;\le t_{-1} \tag{6}$$

$C_a$and N_{max}, in the expressions above, are, respectively, the shear stress amplitude and the maximum normal stress acting on the critical plane. N_{max} is given by

$$N_{max} = N_a + N_m \tag{7}$$

where N_a is the amplitude and N_m the mean value.

The constants μ, k, f, η, λ and α are material parameters, which depend exclusively, as shown in Table 1, on the fatigue limits for fully reversed bending f_{-1} and fully reversed torsion t_{-1}. Applying the McDiamird criterion, one needs to know, in the addition to t_{-1}, the ultimate tensile strength σ_u.

Different from the critical plane approach, the Papadopoulos criterion is applied by simply substituting the applied normal stress and shear stress amplitudes σ_a and τ_a, together with the mean stress σ_m in expression (6). However, one should note that this type of criterion, which is based on the mesoscopic scale approach, is valid for the category of hard metals where the ratio t_{-1} / f_{-1} lies between $1/\sqrt{3}$ and 0,8 [9].

For fully reserved loading, which is the type of loading considered in the present work, σ_m and N_m are taken to be null and consequently N_{max} is to be replaced by N_a and hence inequalities (5) and (6) simplify to

$$\sqrt{(\frac{N_a}{f_{-1}})^2 + (\frac{C_a}{t_{-1}})^2} \;\le \lambda \tag{8}$$

$$\sqrt{\frac{\sigma_a^2}{3} + \tau_a^2} + \alpha \frac{\sigma_a}{3} \;\le t_{-1} \tag{9}$$

Table 1. Definition of the pertinent material constants.

$\mu = 2\left(\frac{t_{-1}}{f_{-1}}\right) - 1$
$k = \frac{2 - (\frac{f_{-1}}{t_{-1}})}{2\sqrt{\frac{f_{-1}}{t_{-1}} - 1}}$
$f = \sqrt{\frac{f_{-1}^2}{4\,(\frac{f_{-1}}{t_{-1}} - 1)}}$
$\eta = \frac{3}{4} + \frac{1}{4}(\frac{\sqrt{3} - \frac{f_{-1}}{t_{-1}}}{\sqrt{3} - 1})$
$\lambda = [cos^2(2\delta)s^2 + sin^2(2\delta)]^{1/2}$
$\alpha = \frac{t_{-1} - (\frac{f_{-1}}{\sqrt{3}})}{\frac{f_{-1}}{3}}$

where $s = t_{-1}/f_{-1}$.

3 Critical plane identification

This can be achieved by first considering a general material plane oriented at angle ψ (Fig.1), where the stress amplitudes N_a and $C_a$acting on such a plane due to applied synchronous in-phase sinusoidal bending and torsion are given by

$$N_a = \frac{1}{2}\,\sigma_a + \frac{1}{2}\,\sigma_a \, cos2\psi + \tau_a sin2\psi \tag{10}$$

$$C_a = |\frac{1}{2}\,\sigma_a \, sin2\psi - \tau_a \, cos2\psi| \tag{11}$$

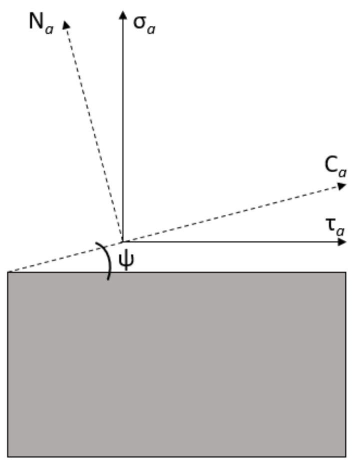

Figure 1: Schematic representation of normal and shear stress amplitudes acting on an arbitrary plane defined by the angle ψ.

Both the Matake and McDiarmid models refer to the critical plane as the plane on which, the shear stress amplitude C_a reaches its maximum. Accordingly the angle $\psi_c$that defines the critical plane orientation is given by

$$tan\psi_c = -\frac{\sigma_a}{2\tau_a} \quad (12)$$

and the corresponding N_a and C_a values can be calculated and then substituted in the left hand side (LHS) of inequalities (1) and (2).

In regard to the Findley model, the critical plane is defined by maximizing the linear combination $(C_a + kN_a)$ and ψ_c in this case will be given by

$$tan2\psi_c = \frac{\sigma_a + 2k\tau_a}{k\sigma_a - 2\tau_a} \quad (13)$$

Again with ψ_c already known, N_a and C_a can be calculated and the LHS of inequality (3) can be determined.

Identification of the critical plane for both C&S and L&M models depend, in the first place, on determining the fracture plane orientation. For a given loading history, the fatigue fracture plane is identified as the material plane normal to the maximum principal stress [5,8]. For a fully reversed loading, the fracture plane is thus oriented at an angle ψ_f given by

$$tan2\psi_f = \frac{-2\tau_a}{\sigma_a} \quad (14)$$

Knowing ψ_f, ψ_c is expressed as [5,8]

$$\psi_c = \psi_f + \delta \quad (15)$$

where δ is given by [5]

$$\delta = \left[1 - \left(\frac{t_{-1}}{f_{-1}}\right)^2\right]\frac{3\pi}{8} \quad (16)$$

for C&S model.

$$\delta = \frac{1}{2}cos^{-1}(A) \quad (17)$$

for L&M model

where $A = \left[\frac{-2+\sqrt{4-4(\frac{1}{s^2}-1)(5-\frac{1}{s^2}-4s^2)}}{2(5-\frac{1}{s^2}-4s^2)}\right]$

Now, with the angle ψ_c already known, one can proceed to apply the C&S and L&M model, substituting N_a and C_a in the LHS of their respective inequalities.

4 Results and discussion

The fracture plane and critical plane orientations, defined by the angle ψ_f, and ψ_c are listed in Tables 2 and 3, in terms of σ_a and τ_a, for the variety of materials indicated in the tables.

Table 2. Fracture and critical plane orientations for different materials, under in phase bend and torsion stresses for Ma, Mc and F models.

			ψ_c (°)		
σ_a(MPa)	**τ_a(MPa)**	**ψ_f (°)**	**Ma**	**Mc**	**F**
Material: Hard steel: f_{-1} = 313.9 MPa; t_{-1} = 196.2 MPa; σ_u = 704.1 MPa					
327.7	**0.0**	0.0	45.0	45.0	37.8
308.0	**63.9**	11.3	56.3	56.3	49.0
255.1	**127.5**	22.5	67.5	67.5	60.3
141.9	**171.3**	33.8	78.8	78.8	71.5
0.0	**201.1**	45.0	0.0	0.0	7.2
Material: Hard steel: f_{-1} = 313.9 MPa; t_{-1} = 196.2 MPa; σ_u = 680.0 MPa					
138.1	**167.1**	33.8	168.8	168.8	176.0
245.3	**122.65**	22.5	157.5	157.5	164.7
299.1	**62.8**	11.4	146.4	146.4	153.6
Material: 42CrMo4: f_{-1} = 398.0 MPa; t_{-1} = 260.0 MPa; σ_u = 1025.0 MPa					
328.0	**157.0**	21.9	156.9	156.9	165.8
233.0	**224.0**	31.3	166.3	166.3	175.2
Material: 34Cr4: f_{-1} = 410.0 MPa; t_{-1} = 256.0 MPa; σ_u = 795.0 MPa					
314.0	**157.0**	22.5	67.5	67.5	60.3
Material: 30NCD16: f_{-1} = 660.0 MPa; t_{-1} = 410.0 MPa; σ_u = 1880.0 MPa					
485.0	**280.0**	24.6	69.6	69.6	62.5
Material: Mild steel: f_{-1} = 235.4 MPa; t_{-1} = 137.3 MPa; σ_u = 518.8 MPa					
245.3	**0.0**	0.0	45.0	45.0	40.2
235.6	**48.9**	11.3	146.3	146.3	51.5
187.3	**93.6**	22.5	157.5	157.5	62.7
101.3	**122.3**	33.8	168.8	168.8	74.0
0.0	**142.3**	45.0	0.0	0.0	4.8
Material: Cast iron: f_{-1} = 96,1 MPa; t_{-1} = 91,2 MPa; σ_u = 230.0 MPa					
93.2	**0.0**	0.0	45.0	45.0	13.1
95.2	**19.7**	11.2	56.2	56.2	24.3
83.4	**41.6**	22.5	157.5	157.5	9.4
56.3	**68.0**	33.8	168.8	168.8	20.7
0.0	**94.2**	45.0	0.0	0.0	31.9

Table 3. Fracture and critical plane orientations for different materials, under in phase bend and torsion stresses for C&S and L&M models.

σ_a(MPa)	τ_a(MPa)	ψ_f (°)	ψ_c (°) C&S	ψ_c (°) L&M
Material: Hard steel: f_{-1} = 313.9 MPa; t_{-1} = 196.2 MPa; σ_u = 704.1 MPa				
327.7	**0.0**	0.0	41.1	39.2
308.0	**63.9**	11.3	52.4	50.5
255.1	**127.5**	22.5	63.6	61.7
141.9	**171.3**	33.8	74.9	73.0
0.0	**201.1**	45.0	86.1	84.2
Material: Hard steel: f_{-1} = 313.9 MPa; t_{-1} = 196.2 MPa; σ_u = 680.0 MPa				
138.1	**167.1**	33.8	74.9	73.0
245.3	**122.65**	22.5	63.6	61.7
299.1	**62.8**	11.4	52.5	50.6
Material: 42CrMo4: f_{-1} = 398.0 MPa; t_{-1} = 260.0 MPa; σ_u = 1025.0 MPa				
328.0	**157.0**	21.9	60.6	58.5
233.0	**224.0**	31.3	70.0	67.9
Material: 34Cr4: f_{-1} = 410.0 MPa; t_{-1} = 256.0 MPa; σ_u = 795.0 MPa				
314.0	**157.0**	22.5	63.7	61.7
Material: 30NCD16: f_{-1} = 660.0 MPa; t_{-1} = 410.0 MPa; σ_u = 1880.0 MPa				
485.0	**280.0**	24.6	66.0	64.2
Material: Mild steel: f_{-1} = 235.4 MPa; t_{-1} = 137.3 MPa; σ_u = 518.8 MPa				
245.3	**0.0**	0.0	44.5	44.1
235.6	**48.9**	11.3	55.8	55.4
187.3	**93.6**	22.5	67.0	66.6
101.3	**122.3**	33.8	78.3	77.9
0.0	**142.3**	45.0	89.5	89.1
Material: Cast iron: f_{-1} = 96,1 MPa; t_{-1} = 91,2 MPa; σ_u = 230.0 MPa				
93.2	**0.0**	0.0	6.7	16.3
95.2	**19.7**	11.2	17.9	27.5
83.4	**41.6**	22.5	29.2	38.8
56.3	**68.0**	33.8	40.5	50.1
0.0	**94.2**	45.0	51.7	61.3

The angle ψ_f, which is invariably determined by the stress amplitudes, is in fact unique for all the models. As can be observed from the same table, the higher the ratio τ_a/σ_a, the higher the angle ψ_f, consistent with the fact that ψ_f tends to zero for uniaxial normal stress and to 45° for pure shear loading.

As one may expect, the critical plane orientation, defined by the angle ψ_c in table, varies from one model to another. Except for the Matake and McDiamird criteria, where the critical plane orientation has the same value of ψ_c, considerable differences can be observed among the other models. These differences are also seen to vary appreciably with the stress amplitudes as well as with the fatigue properties of the material. However, in view of their proper formulation, the C&S and L&M criteria result in essentially the same critical plane orientations, except for a few number of loading conditions associated with the experimental testing of cast iron.

The error index I, associated with the application of any of the six models, refers to the relative difference between the two sides of the inequality. I can thus be expressed as

$$I = \frac{LHS - RHS}{RHS} \times 100 \quad (18)$$

The values of I corresponding to the different loading conditions are listed in Tables 4 and 5, for the variety of materials involved.

Except for a few cases, the vast majority of the I values are situated within the range -10% to 10%, indicating a good predictive capability of the criteria in question. This is also demonstrated by Fig.2, where the overall average values of I are also shown. One can thus conclude that, except for the McDiarmid model, the others are moderately conservative, with the C&S, L&M and P models exhibiting the lowest error compared to the other three.

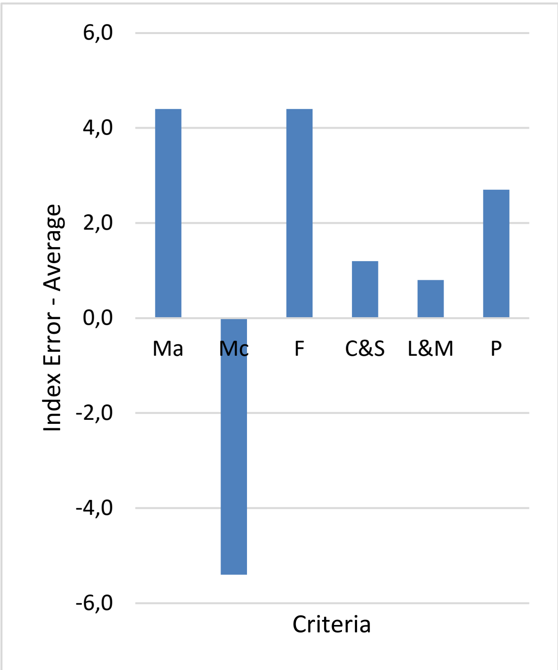

Figure 2: Comparative presentation of the average value of the error index, for the fatigue criteria in question.

 https://doi.org/10.1051/matecconf/201816516013

Table 4: Error index, corresponding Ma, Mc and F criteria.

		Index Error - *I* (%)		
σ_a(MPa)	τ_a(MPa)	Ma	Mc	F
Material: Hard steel: f_{-1} = 313.9 MPa; t_{-1} = 196.2 MPa; σ_u = 704.1 MPa				
327.7	**0.0**	4.4	-4.8	4.4
308.0	**63.9**	4.6	-4.1	4.6
255.1	**127.5**	8.2	1.0	8.2
141.9	**171.3**	3.6	-0.4	3.5
0.0	**201.1**	2.5	2.5	2.5
Material: Hard steel: f_{-1} = 313.9 MPa; t_{-1} = 196.2 MPa; σ_u = 680.0 MPa				
138.1	**167.1**	1.0	-2.8	0.9
245.3	**122.65**	4.0	-2.6	4.0
299.1	**62.8**	1.7	-6.3	1.7
Material: 42CrMo4: f_{-1} = 398.0 MPa; t_{-1} = 260.0 MPa; σ_u = 1025.0 MPa				
328.0	**157.0**	6.8	-4.7	6.7
233.0	**224.0**	10.9	2.8	10.8
Material: 34Cr4: f_{-1} = 410.0 MPa; t_{-1} = 256.0 MPa; σ_u = 795.0 MPa				
314.0	**157.0**	2.0	-3.4	2.0
Material: 30NCD16: f_{-1} = 660.0 MPa; t_{-1} = 410.0 MPa; σ_u = 1880.0 MPa				
485.0	**280.0**	4.7	-3.2	4.7
Material: Mild steel: f_{-1} = 235.4 MPa; t_{-1} = 137.3 MPa; σ_u = 518.8 MPa				
245.3	**0.0**	4.2	1.1	4.2
235.6	**48.9**	7.2	4.3	7.2
187.3	**93.6**	7.8	5.5	7.8
101.3	**122.3**	2.6	1.3	2.5
0.0	**142.3**	3.6	3.6	3.6
Material: Cast iron: f_{-1} = 96,1 MPa; t_{-1} = 91,2 MPa; σ_u = 230.0 MPa				
93.2	**0.0**	-3.0	-38.7	-3.0
95.2	**19.7**	3.4	-33.1	3.4
83.4	**41.6**	5.6	-26.3	5.6
56.3	**68.0**	8.5	-13.2	8.4
0.0	**94.2**	3.3	3.3	3.3

Table 5: Error index, corresponding C&S, L&M and P criteria.

		Index Error - *I* (%)		
σ_a(MPa)	τ_a(MPa)	C&S	L&M	P
Material: Hard steel: f_{-1} = 313.9 MPa; t-1 = 196.2 MPa; σu = 704.1 MPa				
327.7	**0.0**	1.8	4.3	4.4
308.0	**63.9**	1.2	3.3	3.8
255.1	**127.5**	3.1	5.3	5.5
141.9	**171.3**	-1.5	0.3	0.2
0.0	**201.1**	1.9	2.3	2.5
Material: Hard steel: f_{-1} = 313.9 MPa; t-1 = 196.2 MPa; σu = 680.0 MPa				
138.1	**167.1**	-3.9	-2.8	-2.3
245.3	**122.65**	-0.8	1.3	1.4
299.1	**62.8**	-1.5	0.3	0.9
Material: 42CrMo4: f_{-1} = 398.0 MPa; t-1 = 260.0 MPa; σu = 1025.0 MPa				
328.0	**157.0**	0.7	4.5	4.2
233.0	**224.0**	4.1	6.6	7.3
Material: 34Cr4: f_{-1} = 410.0 MPa; t-1 = 256.0 MPa; σu = 795.0 MPa				
314.0	**157.0**	-2.8	-0.8	-0.5
Material: 30NCD16: f_{-1} = 660.0 MPa; t-1 = 410.0 MPa; σu = 1880.0 MPa				
485.0	**280.0**	-0.3	1.1	1.8
Material: Mild steel: f_{-1} = 235.4 MPa; t-1 = 137.3 MPa; σu = 518.8 MPa				
245.3	**0.0**	3.9	4.0	4.1
235.6	**48.9**	5.9	6.0	6.3
187.3	**93.6**	4.7	5.0	5.0
101.3	**122.3**	-1.0	-1.0	-0.8
0.0	**142.3**	3.6	4.0	3.6
Material: Cast iron: f_{-1} = 96,1 MPa; t-1 = 91,2 MPa; σu = 230.0 MPa				
93.2	**0.0**	-3.6	-13.9	-3.0
95.2	**19.7**	2.5	-26.3	2.8
83.4	**41.6**	4.0	4.8	3.8
56.3	**68.0**	5.4	6.8	5.9
0.0	**94.2**	-1.7	2.7	3.3

5 Conclusion

Based on what is presented above, the following conclusions can be drawn

- Fracture plane orientation, in fully reversed multiaxial fatigue loading, is exclusively determined by the ratio between the shear and normal stress amplitudes.
- For a given loading condition, the critical plane orientation depends on the adapted multiaxial fatigue criterion. Whereas the Matake and McDiarmid models possess the same critical plane, the C&S and L&M models indicate critical planes with orientations that are close to each other.
- Critical plane orientation predicted by the Findley criterion is generally close to that defined by the Matake model.
- The overall average of the error index I is limited to -5,5% ≤ I ≤ 4,5%, indicating reasonable predictive capability of the models in question in defining fatigue behavior.
- Except for the McDiarmid criterion, the models are seen to be conservative as they mostly exhibit positive I values.

This work was developed within the scope of the Research and Technological Development of the Brazilian Electric Energy Sector Program regulated by ANEEL, with the support of the Eneva Companies - Pecém II Energy Generation S.A., Itaqui Energy Generation S.A. and Paranaíba I, II and III Energy Generation S.A.

References

1. T. Matake, *An explanation on fatigue limit under combined stress*, Bull JSME **20**, 257 (1977)
2. DL. McDiamid, *Fatigue under out of phase bending and torsion,* Fat. Fract. Engng. Mater. Struct **9**, 457 (1987)
3. DL. Mc Diarmid, *A general criterion for high cycle multiaxial fatigue failure*, Fat. Fract. Engng. Mater. Struct **14**, 429 (1991)
4. WN. Findley, *A theory for the effect of mean stress on fatigue of metals under combined torsion and axial load or bending*, J. Engng. Ind. Trans. ASME **81**, 301 (1959) (Cited in reference 5)
5. A. Carpinteri, A. Spagnoli, *Multiaxial high-cycle fatigue criterion for hard metals*, Int. J. Fat. **23**, 135 (2001)
6. A. Carpinteri, A. Spagnoli, S. Vantadori, *Multiaxial fatigue assessment using simplified critical plane-based criterion,* Int. J. Fat. **33**, 969 (2011)
7. A. Carpinteri, A. Spagnoli, S. Vantadori, C. Bagnic, *Structural integrity assessment of metallic components under multiaxial fatigue: the C-S criterion and its evolution,* Fat. Fract. Engng. Mater. Struct **36**, 870 (2013)
8. Y. Liu, S. Mahadevan, *Multiaxial high-cycle fatigue criterion and life prediction for metals*, Int. J. Fat. **27**, 870 (2005)
9. IV. Papadopoulos, P. Davoli, C. Gorla, M. Fillipini, A. Bernarconi, *A comparative study of multiaxial high-cycle fatigue criteria for metals*, Int. J. Fat. **19**, 219 (1997)
10. IV. Papadopoulos, *Long life fatigue under multiaxial loading*, Int. J. Fat. **23**, 839 (2001)
11. T. Nishihara, M. Kawamoto, *The strength of metals under combined alternating bending and torsion with phase difference*, Mem College Eng., Kyoto Imper. Univ. **11**, 85 (1945) (Reported in reference 5)
12. H. Zenner, R. Heindenreich, IZ. Richter Werkstofftech, **16**, 101 (1985) (Reported in reference 9)